Proteins as nano-machines: dynamics–function relations studied by neutron scattering

2003 J. Phys.: Condens. Matter 15 S1673

(http://iopscience.iop.org/0953-8984/15/18/301)

INSTITUTE OF PHYSICS PUBLISHING JOURNAL OF PHYSICS: CONDENSED MATTER

J. Phys.: Condens. Matter **15** (2003) S1673–S1682 PII: S0953-8984(03)54865-2

Proteins as nano-machines: dynamics–function relations studied by neutron scattering

Giuseppe Zaccai[1]

Institut de Biologie Structurale CEA-CNRS and Institut Laue-Langevin, 41 rue Jules Horowitz, 38027 Grenoble Cedex 1, France

E-mail: zaccai@ibs.fr

Received 16 October 2002
Published 28 April 2003
Online at stacks.iop.org/JPhysCM/15/S1673

Abstract

A protein is a nano-machine whose molecular structure was selected by evolution to perform specific biological functions. Neutron spectroscopy is uniquely suited to provide experimental data on atomic motions in a protein under the influence of forces that maintain its stable and active molecular structure. Experiments are reviewed relating such a dynamics to soluble protein folding and stability in different environments, and to the activity of bacteriorhodopsin, a membrane protein nano-machine with light-driven proton pump activity.

1. Introduction: protein structure, dynamics and function

1.1. Folding[2]

It is essential to distinguish between a protein (the biologically active substance selected by evolution) and its chemical composition, the polypeptide chain, a polymeric sequence of amino acid residues. The sequence, or primary structure, of a given protein is encoded in its DNA gene. The resulting polypeptide chain is linear, unbranched and of well-defined length (i.e. with a fixed number of residues). A normal synthetic polymer solution contains a statistical distribution of chain lengths and conformations. In contrast, a 'pure' (i.e. containing one type of protein) protein solution (typically about 10^{15} molecules) contains polypeptide chains that are all identical in molecular mass. This has been confirmed in a spectacular manner by mass spectrometry with a sensitivity of one atomic mass unit in 10^5. In order to attain its active protein conformation, the polypeptide chain folds under particular environmental conditions into a unique three-dimensional structure (the tertiary structure; secondary structure elements denote local conformations such as alpha helices or beta sheets that associate to form the

[1] Author to whom any correspondence should be addressed.

[2] There are few references to original work in this section, because the information presented can be found in any modern biochemistry textbook.

tertiary structure). The pure solution of protein molecules, therefore, is mono-disperse not only in molecular mass, but also in three-dimensional structure.

Genetic information is one dimensional but biological activity resides in the three-dimensional structure. The thermodynamics of protein folding would have been straightforward if the polypeptide chain folded in vacuum. Considering the free energy change for the unfolded-to-folded transition:

$$\Delta G_{uf} = \Delta H_{uf} - T\,\Delta S_{uf},$$

both the enthalpy and entropy changes are negative due, respectively, to intra-chain bonding (e.g. hydrogen bonds) and the loss of configurational freedom upon folding. Below a melting temperature, T_m, at which $\Delta H_{uf} = T_m\,\Delta S_{uf}$, the folded form will be favoured; above, the protein unfolds. Under physiological conditions, however, a protein folds in a specific environment: aqueous solvent if it is soluble, lipid if it is a membrane protein. Various interactions occur within the chain and between the chain and solvent components: water molecules, lipids, ions and other small solutes. The loss of chain configurational freedom upon folding may be more than compensated for by the loss of configurational freedom of water molecules around exposed apolar groups, which cannot form hydrogen bonds, in the unfolded chain (the hydrophobic effect). Because of the presence of the solvent, therefore, each of ΔH_{uf} and $T\,\Delta S_{uf}$ may be negative, positive or even zero. Also, more bonds may be formed between the unfolded chain and its environment than within the folded structure.

An important experimental result from calorimetric studies of protein folding (reviewed in [1]) is the inverted bell-shaped ΔG_{uf} versus T curve, arising from compensation between negative and positive contributions to the enthalpy and entropy changes. The folded form of a protein is favoured in a restricted temperature range. The protein unfolds at the low-temperature end of the range (cold unfolding) as well as at the high-temperature end. The energy of stabilization, given by the maximum value of $|\Delta G_{uf}|$, has been measured for globular proteins to be about 10 kcal mol^{-1}. Note that this is equivalent to the enthalpy change for the formation of one or two hydrogen bonds, when hundreds are formed or broken upon folding! The low value of the stabilization energy results from the difference between terms that are orders of magnitude larger and illustrates perfectly the difficulty (or impossibility) of calculating protein folding from *ab initio* theoretical considerations. The approximations applied, because of the diversity and complexity of the interactions involved (especially those relating to the solvent), would lead to uncertainties that are significantly larger than the effects to be predicted.

Reasonably reliable protein structure predictions from gene sequences have been based on homology modelling. Homologous proteins display the same biological function in different organisms and have evolved from a common ancestor. It is a good assumption, in general, that homologous proteins share a common three-dimensional structure even if there are large variations in their primary structures. A structure solved experimentally (by x-ray crystallography or NMR) for one member of the family serves as a basis for modelling the others.

1.2. Energy landscape

From a careful analysis of experimental data on carbon monoxide binding to myoglobin, Frauenfelder and collaborators proposed a model for the free energy versus conformational coordinate surface (the energy landscape) of a folded protein in terms of conformational substates (CS) (review in [2]). The surface is multi-dimensional with as many dimensions as coordinates to describe a particular conformation. The CS correspond to free energy minima that may differ from each other by less than k_BT (k_B is Boltzmann's constant) at

physiological temperatures, so that the protein dynamically samples different conformations. At low temperatures, each protein molecule in an ensemble will be 'frozen' into one of the CS. Contrary to what was written above, therefore, the three-dimensional structure of the protein is not strictly unique. Structural differences between the CS, however, are expected to be small (e.g. different rotation angles for certain amino acid side-chains [3]) and the overall folding of the protein is maintained.

1.3. Evolution, the dynamics–function relation and neutrons

The 'structure–function relation' lies at the heart of molecular biology. It describes a more subtle hypothesis than a simple statement that an enzyme has a structure that allows it to catalyse a certain reaction. This would suggest that the hypothesis could be applied to copper, for example, whose electronic structure provides it with the useful property of being a good conductor. Copper does not *exist* because it is a good conductor, when, in fact, the enzyme *exists* only because of its catalytic function. A protein structure exists today because it has been selected by evolution. And it has been selected by evolution because of properties that allow it to perform a particular biological function. When evidence became available of the importance of protein dynamics for function (i.e. that appropriate flexibility was required and a 'frozen' protein was inactive even though it had the correct structure), the hypothesis was extended to include dynamics and authors wrote of the 'structure–dynamics–function relation'. I pointed out, however, that dynamics pertains to forces and not just to motions [4] and, since forces underlie both protein structure and internal motions, the fundamental relation in molecular biology is the 'dynamics–function' relation. Evolution, in fact, selects dynamics. A mutation at the gene level will be accepted or rejected according to its effect on the energy landscape of the protein.

The forces that maintain a biological macromolecule folded and active are known: hydrogen bonds, screened electrostatic interactions, van der Waals interactions, hydrophobic interactions (the 'insolubility' of apolar groups in water). They are weak forces in that their associated energy is close to k_BT at physiological temperature (∼meV). The atomic fluctuations for protein internal motions associated with these forces are in the ångström range. Thermal and cold neutrons constitute particularly useful radiation probes for studying molecular dynamics in proteins and its relation to biological function and activity. Their wavelengths (∼Å) and energies (∼meV) correspond to the fluctuations and energy of thermal excitations, respectively, so neutrons are sensitive simultaneously to the amplitudes and frequencies of internal molecular motions. They penetrate deeply into biological samples with negligible radiation damage. A large hydrogen–deuterium isotope effect makes neutrons very powerful for studying components within complex systems that can be selectively labelled. Neutron experiments carried out to study protein dynamics have been reviewed recently [5].

2. Neutron scattering

2.1. Neutron scattering functions

Neutron scattering is analysed in terms of the scattering vector ($\boldsymbol{Q}$) and energy transfer ($h\omega$). The differential scattering cross-section of a sample of N identical atoms is given by

$$\frac{\partial^2\sigma}{\partial\Omega\,\partial\omega} = N\hbar\frac{k'}{k}b^2S(\boldsymbol{Q},\omega) \tag{1}$$

where Ω is the solid angle, b is the nuclear scattering length of the atoms, $\boldsymbol{k}$, $\boldsymbol{k}'$ ($k = k' = 2p/\hbar$) are incident and scattered wavevectors, respectively, and the energy transfer and momentum

transfer to the neutron during the scattering process are, respectively,

$$\Delta E = h\omega$$
$$\Delta \boldsymbol{p} = \hbar(\boldsymbol{k}' - \boldsymbol{k}) = \hbar \boldsymbol{Q}.$$

The scattering function (or dynamic structure factor) $S(\boldsymbol{Q}, \omega)$ is written as

$$S(\boldsymbol{Q}, \omega) = \frac{1}{2\pi} \int_{-\infty}^{+\infty} I(\boldsymbol{Q}, t) \exp\{-\mathrm{i}\omega t\} \, \mathrm{d}t. \tag{2}$$

The intermediate-scattering function

$$I(\boldsymbol{Q}, t) = \frac{1}{2\pi} \int_{-\infty}^{+\infty} g(\boldsymbol{r}, t) \exp\{-\mathrm{i}\boldsymbol{Q} \cdot \boldsymbol{r}\} \, \mathrm{d}\boldsymbol{r} = \frac{1}{N} \sum_{k,j} \langle \mathrm{e}^{\mathrm{i}\boldsymbol{Q} \cdot \boldsymbol{r}_k(t)} \mathrm{e}^{-\mathrm{i}\boldsymbol{Q} \cdot \boldsymbol{r}_j(0)} \rangle \tag{3}$$

is the space Fourier transform of the atomic correlation function (where the angle brackets indicate thermal averaging), N being the number of scattering centres in the sample:

$$g(\boldsymbol{r}, t) = \frac{1}{N} \sum_{k,j}^{N} \langle \delta\{\boldsymbol{r} + \boldsymbol{r}_k(0) - \boldsymbol{r}_j(t)\} \rangle. \tag{4}$$

The expression $b^2 S(\boldsymbol{Q}, \omega)$ can be split into two terms after summation and thermal averaging over all atoms and spin states, one part being the sum of terms from individual nuclei (incoherent contribution), the other one containing only mixed terms (coherent contribution):

$$\frac{\mathrm{d}^2\sigma}{\mathrm{d}\Omega \, \mathrm{d}\omega} = \frac{1}{2\pi\hbar} \frac{k'}{k} \int_{-\infty}^{+\infty} \left\{ \sum_k b_{inc}^2 \langle \mathrm{e}^{\mathrm{i}\boldsymbol{Q} \cdot [\boldsymbol{r}_k(0) - \boldsymbol{r}_k(t)]} \rangle + \sum_{k,j}^{k \neq j} b_{coh}^2 \langle \mathrm{e}^{\mathrm{i}\boldsymbol{Q} \cdot [\boldsymbol{r}_k(0) - \boldsymbol{r}_j(t)]} \rangle \right\} \exp(-\mathrm{i}\omega t) \, \mathrm{d}t. \tag{5}$$

The coherent part of the scattered intensity results from the interference of waves scattered by different nuclei; the incoherent part is the difference between the total scattering and the coherent part. Incoherent scattering can be understood as waves scattered by individual atoms and interfering only with themselves during a time course that is defined in practice by the instrumental resolution.

H has the highest incoherent cross-section of all nuclei usually present in biological samples. The spin dependence of the neutron–nucleus interaction lies at the origin of incoherent scattering. The neutron and the nucleus with which it interacts have intrinsic spins. During the scattering event, the compound neutron–nucleus system can be described by a composite spin quantum number, and the effective scattering length depends on whether or not the spins are aligned. When sample and beam are unpolarized (the case in all experiments described below), the mean scattering length value corresponds to the coherent scattering length, whereas the incoherent scattering length results from the deviation from the mean.

Neutron scattering from a non-crystalline biological sample is dominated by the incoherent contribution of hydrogen. In the space–time window examined by energy-resolved neutron scattering experiments, the individual motions of the H atoms reflect the larger groups (e.g. amino acid side-chains in proteins) to which they are bound. Such experiments, therefore, provide a very good probe of macromolecular internal dynamics.

The scattered intensity as a function of energy transfer can be divided into elastic scattering (ω smaller than instrumental resolution), quasi-elastic scattering (broadening of the elastic peak) and inelastic scattering (for ω-peaks outside the elastic peak), each component corresponding to particular types of motion in the sample. Elastic scattering provides information in terms of fluctuation values on all motions occurring in a time interval defined by instrumental energy resolution (typically ~0.1–1 ns). Quasi-elastic scattering provides

information in terms of fluctuation values and correlation times of diffusional motions. Inelastic scattering provides information in terms of fluctuation values and frequencies of vibrational modes.

Neutron scattering from biological samples is quite weak, and in my laboratory we decided to concentrate on elastic scattering experiments. They present the highest signal-to-noise ratios, thus allowing one to examine a wider variety of samples under various experimental conditions.

2.2. Localized motions and the Guinier approximation

The total elastic intensity (within instrumental resolution) as a function of scattering vector contains information on the geometry of motions integrated over the time corresponding to the instrumental resolution, provided that the motions are localized (i.e. well inside the space window defined by the scattering vector range). For example, if H-atom motions sweep out an ellipse in 100 ps, the elastic scattered intensity will correspond to the scattering of an ellipse provided that the instrumental resolution corresponds to a time of 100 ps or longer (energy resolution of about 10 μeV or better).

As the nuclear positions after a long time, $r_k(\infty)$, are uncorrelated to the initial positions, $r_k(0)$, for infinitely good energy resolution ($\omega = 0$), the total elastic intensity is described by the time-independent part of the intermediate-scattering function:

$$I_{inc}(\boldsymbol{Q}, \infty) = \frac{1}{N} \sum_k |\langle e^{i\boldsymbol{Q}\cdot r_k} \rangle|^2. \tag{6}$$

In the Gaussian approximation, the Fourier transform of equation (6) is

$$S_{inc}(\boldsymbol{Q}, \omega = 0) = \exp\left[-\tfrac{1}{6}\langle u^2 \rangle Q^2\right]. \tag{7}$$

It is valid for the product $\langle u^2 \rangle Q^2$ small, where $\langle u^2 \rangle$ is the atomic mean square displacement. From (21), we obtain

$$\langle u^2 \rangle = -6 \left. \frac{\mathrm{d} \ln[S(\boldsymbol{Q}, \omega = 0)]}{\mathrm{d}(Q^2)} \right|_{Q=0}. \tag{8}$$

Note the similarity of this formulation to the Guinier approximation in small-angle scattering, with $\langle u^2 \rangle / 2$ equal to the radius of gyration squared. In both interpretations of small-angle scattering and elastic neutron scattering as a function of scattering vector, the assumption is that there is interference for waves scattered from within a 'particle' (the macromolecule in solution and the H nucleus moving in time, respectively) and no interference between 'particles'.

2.3. The elastic scan, mean squared displacements and resilience

An elastic scan is a plot of $\langle u^2 \rangle$ calculated from equation (8) as a function of temperature. An elastic scan of a myoglobin powder measured on a spectrometer with 8 μeV resolution, corresponding to a time window of about 0.1 ns, is shown in figure 1 [6, 7]. The break in the $\langle u^2 \rangle$ versus T line at about 200 K is a dynamical transition that has been observed for several hydrated protein powders and membranes and interpreted according to different physical models [8, 9]. Briefly, the dynamical transition is from a harmonic regime at lower temperatures where $\langle u^2 \rangle$ is linear with T and extrapolates to zero-point motion at $T = 0$ (e.g. in the CS model, the protein is trapped in a CS) to an anharmonic regime above the transition (where, in the CS model, the problem would sample different CS).

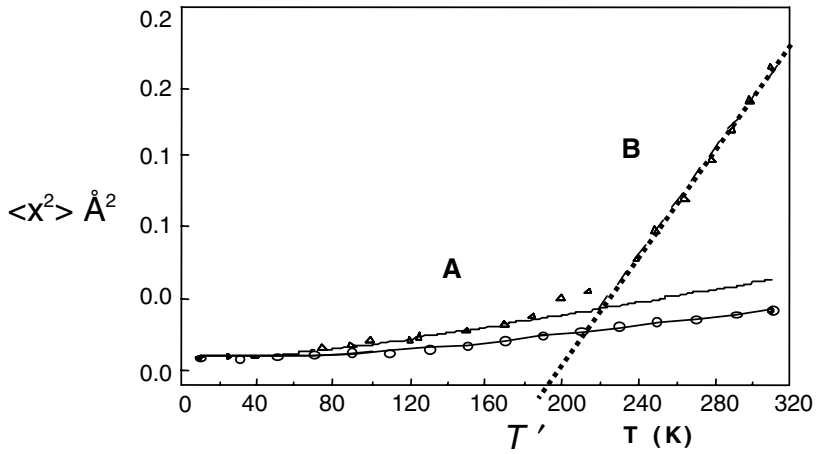

Figure 1. Elastic scans of a myoglobin powder hydrated in D_2O [6] and in a trehalose glass [7]. Mean squared fluctuations expressed as $\langle x^2\rangle = \langle u^2\rangle/6$ (compare equation (7)) are plotted as a function of temperature. The straight line approximations and the corresponding force constant values calculated from equation (9) are $\langle k\rangle = 3$ N m^{-1} for line A and 0.3 N m^{-1} for line B. The D_2O-hydrated sample shows a dynamical transition from a harmonic to a non-harmonic regime at about T'; the trehalose sample is maintained in its harmonic state to beyond room temperature.

An effective force constant $\langle k'\rangle$ associated with protein resilience has been introduced to quantify the temperature dependence of the $\langle u^2\rangle$ values [4]:

$$\langle k'\rangle = 2k_B\left(\frac{\mathrm{d}\langle u^2\rangle}{\mathrm{d}T}\right)^{-1}. \tag{9}$$

In the harmonic regime, $\langle k'\rangle$ corresponds to a properly defined mean force constant for a set of harmonic oscillators. Above the dynamical transition the measured $\langle k'\rangle$ value corresponds to a force constant in a quasi-harmonic approximation, or can be related to a model force constant calculated in a two-potential-well model (a simplification of a CS energy landscape), for example (figures 1 and 2). The mean force constant values given in figure 1 show how coating myoglobin in a trehalose glass stiffens the protein by a factor of 10 and inhibits the dynamical transition, providing an explanation for the strong protective effect of trehalose on protein structures.

3. Environmental adaptation and dynamics–stability relations

3.1. Halophilic malate dehydrogenase 'adapts' to its solvent environment

Malate dehydrogenase from *Haloarcula marismortui* (*Hm*MalDH) is a *halophilic* protein in that it requires molar salt concentrations in its solvent in order to be stable and soluble [10]. It has been studied extensively and has different stability behaviours in H_2O and D_2O solutions containing either NaCl or KCl [11]. Mean squared atomic fluctuations on the 0.1 ns timescale were calculated from protein solutions in the temperature range 280–320 K (to avoid solvent freezing conditions). Effective force constants were calculated from the variation of the mean squared fluctuation with temperature. The resilience of *Hm*MalDH increased progressively with increasing stability (measured by the unfolding or aggregation temperature for each solvent condition), from molar NaCl in H_2O ($\langle k'\rangle = 0.1$ N m^{-1}), via molar KCl in D_2O ($\langle k'\rangle = 0.2$ N m^{-1}) to molar NaCl in D_2O ($\langle k'\rangle = 0.5$ N m^{-1}). The higher stability

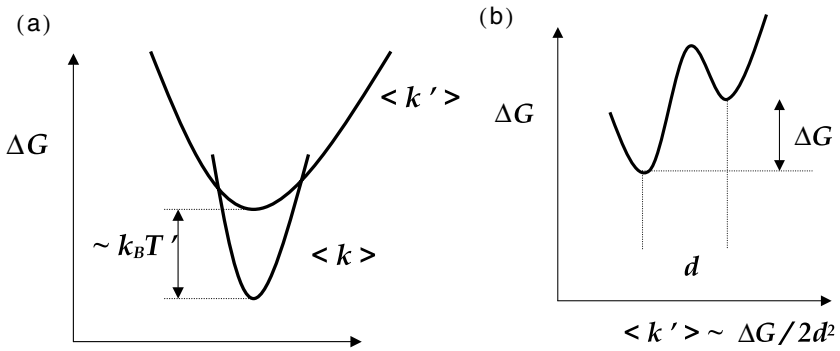

Figure 2. Quasi-harmonic (a) and two-well potentials (b), showing the correspondence to the effective force constants, $\langle k' \rangle$, calculated from the various slopes of the elastic scans in figure 1 (see also equation (9)).

is associated with increased rigidity showing the dominance of enthalpic terms arising from bonded interactions. It was suggested that these are associated with hydrated ion binding that had been shown previously to stabilize the halophilic protein in high-salt solvents [12].

3.2. Dynamics of unfolded states

The rate of protein folding is determined by the dynamics in its potential energy landscape. While the energy landscape of protein folding has been the subject of intense study, there are few experimental data on the dynamics of unfolded proteins and partially folded intermediates such as the so-called molten globule.

Incoherent quasi-elastic neutron scattering (QENS) experiments were performed on unfolded yeast phosphoglycerate kinase [13]. By applying a model of diffusion in a sphere of radius a, the experiments revealed an increase in the population of H atoms participating in the picosecond timescale diffusive internal dynamics, from approximately 60% in the native protein to more than 80% in the denatured protein. The radius of the sphere also increased, from approximately 1.8 Å in the native protein to approximately 2.2 Å in the denatured protein.

The internal dynamics of native bovine alpha-lactalbumin (BLA), its molten globule (MBLA) and denatured (unfolded) states have been examined by means of QENS [14, 15]. The results showed length-scale-dependent picosecond dynamics. On the shorter length scales, the mean potential barrier to local jump motions is higher in BLA than in MBLA. On longer length scales, localized diffusive motions are more restricted in BLA than in MBLA. BLA and MBLA states have similar mean square amplitudes for high-frequency motions, showing that bond vibrational motions do not change significantly upon folding. Interestingly, the quasi-elastic scattering intensities suggested that 'clusters' of atoms are moving collectively within the proteins on picosecond timescales, with a shorter correlation length or 'cluster size' in the molten globule (6.9 Å) than in BLA (18 Å). QENS experiments on DBLA also suggested that there are still secondary and tertiary structure elements fluctuating on subnanosecond timescales in the denatured protein. Three dynamics regimes were found based on the length scale dependence of the measured correlation functions. When $0.05 < Q < 0.5$ Å^{-1}, the dynamic behaviour is similar to that of a random coil. However, when $0.5 < Q < 1.0$ Å^{-1}, the effective diffusion constant decreases with increasing Q, a striking dynamic behaviour that is not found in any chain-like macromolecule. The authors suggested that this unusual dynamics is due to the presence of a strongly attractive force and collective conformational

fluctuations in both the native and the denatured states of the protein. Above $Q > 1.0$ Å^{-1} the dynamics reflects the behaviour of individual residues. As with the molten globule, the potential barrier for side-chain jump motions in the denatured protein is reduced in the denatured protein compared to the native protein. The results taken together support the view that secondary and tertiary structure clusters are established in the early stages of protein folding.

4. Dynamics–activity relations

4.1. Bacteriorhodopsin in the purple membrane: a light-driven nano-machine

The purple membrane (PM) patches in the cell membrane of the halophile *Halobacterium salinarum* are made up of bacteriorhodopsin (BR), a retinal binding protein, organized with specific lipids on a highly ordered hexagonal two-dimensional lattice. Rhodopsin is the retinal binding protein in the human eye and BR was so named because it was the first retinal binding protein to be discovered in a micro-organism. BR spans the membrane from side to side in seven alpha helices. The retinal molecule is bound to the side-chain of a lysine residue close to the membrane thickness centre, on the seventh helix. The absorption maximum (colour) of the chromophore is strongly dependent on its close environment. Free retinal is yellow with an absorption maximum at about 400 nm. When it is bound to BR, the absorption maximum shifts to 565 nm, giving the membrane its purple colour. Upon absorption of a photon, the retinal conformation changes in picoseconds, following a femtosecond electronic rearrangement. Light energy is converted to mechanical energy, which couples with thermal excitations in the protein. There results a relaxation on the millisecond timescale in several steps, with a proton being released by the protein on the extracellular side of the membrane, and a proton bound on the cytoplasmic (CP) side. The proton transfer is against the chemical potential, so the BR nano-machine is a light-activated proton pump. Each step of the relaxation process is characterized by a specific environment and absorption maximum for the retinal, giving rise to a *photocycle* that has been studied extensively by spectroscopy. The photocycle provides biophysics with a very sensitive measure of BR activity. The challenge is to understand the detailed mechanisms of the BR nano-machine by relating spectroscopic observations with membrane structure and dynamics. Neutron diffraction and spectroscopy experiments, making use of hydrogen–deuterium labelling to focus on different parts of the complex system (hydration, protein components, lipids), continue to play an important role in meeting this challenge [16].

4.2. Hydration, the photocycle and dynamics

The relationship between dynamics and BR activity was explored through their hydration dependence, by neutron scattering and photocycle experiments, respectively. BR conformational changes (on the millisecond timescale) associated with proton pump activity are inhibited below a critical hydration level obtained in a 60% relative humidity atmosphere at room temperature. Neutron scattering experiments indicated that there was a similar threshold for anharmonic picosecond-to-nanosecond fluctuations, confirming that fast thermal dynamics acts as the 'lubricant' for millisecond structural reorganizations in proteins. A first set of neutron elastic scans with an energy resolution of 8 μeV (corresponding to an about 100 ns time window) were performed on two extreme hydration states of PM (dry and hydrated at 93% relative humidity). A dynamical transition at about 230 K between a harmonic and a non-harmonic dynamics regime was observed only for the hydrated membrane. Since the BR photocycle can be completed only in the hydrated PM, above 230 K, a strong correlation

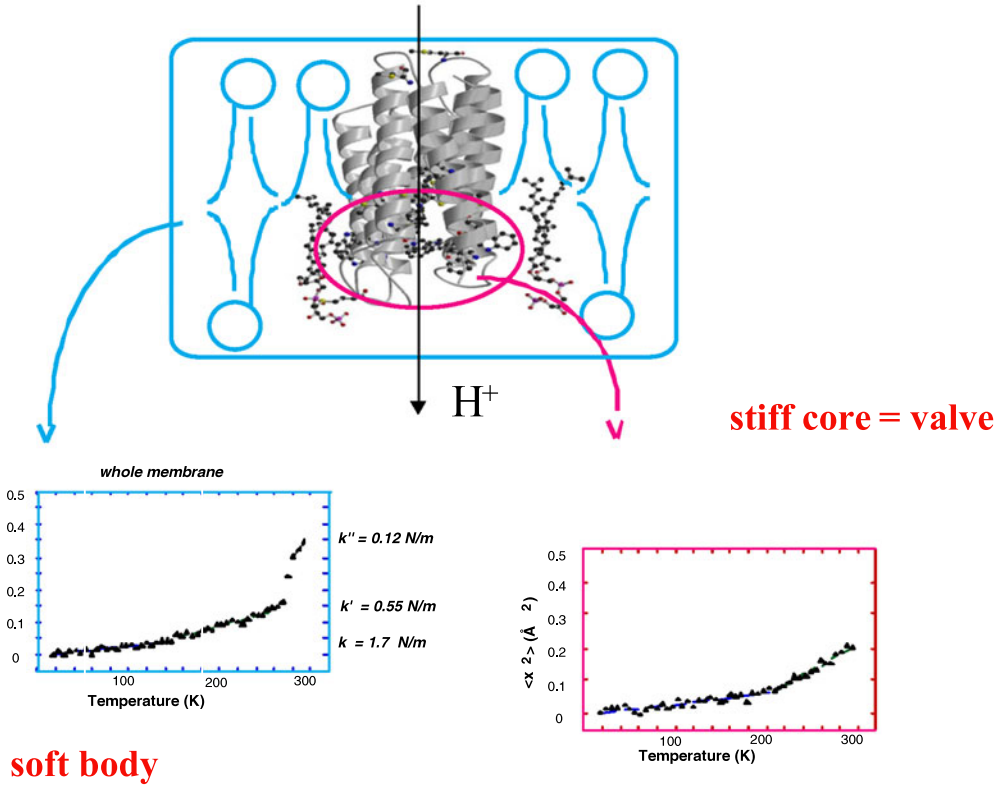

Figure 3. A schematic side-view of BR in the PM. The protein is shown as a ribbon diagram (from data deposited in the protein data bank [20]). The labelled amino acid residues and a glycolipid molecule on the extracellular (EC) side are shown in ball-and-stick representation. The other lipids are represented as ellipses (for the head-groups) and curves (for the tails). The CP side of the membrane is at the top, the EC side at the bottom. Mean square fluctuation data and the effective force constants calculated, respectively, for the system globally (unlabelled sample) and for the active core of the protein that surrounds the proton switch or valve (H-labelled Trp, Met and retinal in an otherwise deuterated membrane) are shown below the molecular model (from [19]).

(This figure is in colour only in the electronic version)

was shown to exist between the non-harmonic dynamics and activity. The dry membrane is harmonic and inactive over the entire temperature range of the measurements. The results supported the hypothesis that a globally soft environment obtained through the action of both temperature and hydration is required to ensure BR activity. Further neutron elastic scans in different Q-ranges (length scales) and quasi-elastic scattering experiments provided evidence of populations of motions characterized by different mean square amplitudes, different correlation times and with dynamical transitions at different temperatures [17, 18]. Interestingly, each population responded in a different way to hydration. The results quantified the dynamical heterogeneity of the membrane and further analysis should allow correlation of the different dynamic populations with specific steps in the photocycle.

4.3. H–D labelling shows the specific internal dynamics

The neutron scattering experiments showed that BR has to be globally soft in order to function as a proton pump. Any pump requires a valve in its structure, to ensure unidirectional flow of

the pumped material. In the case of BR, the valve is the Schiff base linkage of the retinal to the protein, which acts as a switch. It releases a proton towards the EC part of the protein, in the middle of the photocycle, then turns to accept one from a donor on the CP side. Neutron scattering experiments were performed on deuterium-labelled PM in order to address the question of whether or not globally soft active BR had a more rigid core, which would control the stereo-specific selection of retinal conformations that act as the proton pump valve.

Fully deuterated PM, except for hydrogenated retinal methionine and tryptophan residues in the BR, was prepared by *in vivo* biosynthesis in *H. salinarum* cultures [19]. The selected groups cluster in the retinal binding pocket and the EC moiety of BR. Elastic scans on the labelled membranes confirmed that, as expected from its valve function, the core of BR is significantly more resilient than PM globally (figure 3).

5. Conclusions and perspectives in the post-genome-sequencing era

A biologically functional protein has been selected by evolution on the basis of its structure, its stability and motional flexibility on various timescales—aspects that result from the forces that act in the folded protein. Evolution selects dynamics and the challenge is to devise experimental methods to characterize internal molecular forces and their correlation with the genome sequence, on the one hand, and biological activity, on the other. So far, neutron scattering experiments have been performed mainly on isolated systems, membranes being the more complex representatives. The observed dependence of the dynamics on the environment, however, is an important general result of the experiments. It should stimulate the development of methods for characterizing the dynamics in conditions of complexity that are as close to *in vivo* conditions as possible. Because the analysis is based on incoherent scattering, there are no stringent requirements for sample preparation and H motions in complex systems can be examined easily. Recently, data were collected for whole cells to compare psychrophilic (living at 4 °C), mesophilic (living at 37 °C) and thermophilic (living at 75 °C) organisms in order to characterize mean protein dynamics as a function of adaptation temperature [21].

References

[1] Makhatadze G I and Privalov P L 1995 *Adv. Protein Chem.* **47** 307–425
[2] Frauenfelder H and McMahon B 1998 *Proc. Natl Acad. Sci. USA* **95** 4795–7
[3] Declercq J P, Evrard C, Lamzin V and Parello J 1999 *Protein Sci.* **8** 2194–204
[4] Zaccai G 2000 *Science* **288** 1604–7
[5] Gabel F, Bicout D, Lehnert U, Tehei M, Weik M and Zaccai G 2002 *Q. Rev. Biophys.* **35** 327–67
[6] Doster W, Cusack S and Petry W 1989 *Nature* **337** 754–6
[7] Cordone L, Ferrand M, Vitrano E and Zaccai G 1999 *Biophys. J.* **76** 1043–7
[8] Parak F, Knapp E W and Kucheida D 1982 *J. Mol. Biol.* **161** 177–94
[9] Parak F 2003 *Rep. Prog. Phys.* **66** 103–29
[10] Madern D, Ebel C and Zaccai G 2000 *Extremophiles* **4** 91–8
[11] Bonneté F, Madern D and Zaccai G 1994 *J. Mol. Biol.* **244** 436–47
[12] Tehei M, Madern D, Pfister C and Zaccai G 2001 *Proc. Natl Acad. Sci. USA* **98** 14356–61
[13] Receveur V, Calmettes P, Smith J C, Desmadril M, Coddens G and Durand D 1997 *Proteins: Struct. Funct. Genet.* **28** 380–7
[14] Bu Z, Neumann D A, Lee S-H, Brown C M, Engelman D M and Han C C 2000 *J. Mol. Biol.* **301** 525–36
[15] Bu Z, Cook J and Callaway J E 2001 *J. Mol. Biol.* **312** 865–73
[16] Zaccai G 2000 *Biophys. Chem.* **86** 249–57
[17] Lehnert U, Réat V, Weik M, Zaccai G and Pfister C 1998 *Biophys. J.* **75** 1945–52
[18] Fitter J, Ernst O P, Hauss T, Lechner R E, Hofmann K P and Dencher N A 1998 *Eur. Biophys. J.* **27** 638–45
[19] Réat V, Patzelt H, Pfister C, Ferrand M, Oesterhelt D and Zaccai G 1998 *Proc. Natl Acad. Sci. USA* **95** 4970–5
[20] Girgorieff N, Ceska T A, Downing K H, Baldwin J M and Henderson R 1995 *J. Mol. Biol.* **259** 393–421
[21] Zaccai G *et al* 2003 private communication